

# EFFECT OF BIAXIALITY ON THE FATIGUE PERFORMANCE OF A LAMINATED COMPOSITE

Raghuram Mandapati<sup>1</sup> and P. K. Mallick<sup>1</sup>

<sup>1</sup>. University of Michigan-Dearborn, 4901 Evergreen Road, Dearborn, MI 48128, USA  
email: [raghuram@umich.edu](mailto:raghuram@umich.edu) and [pkm@umich.edu](mailto:pkm@umich.edu)  
webpage: <https://umdearborn.edu/cecs/research/centers>

**Keywords:** Laminated plates, biaxial fatigue, biaxiality ratio, fatigue damage, stiffness degradation

## ABSTRACT

This paper will present biaxial fatigue data of  $[0/90/0_4/\bar{0}]_s$  E-glass/epoxy laminates under a combination of normal and shear loadings. A butterfly-shaped Arcan specimen was developed and used for fatigue testing. Four different fiber orientations in the outer layers were considered, namely 0, 30, 45 and 90°. A variety of combinations of shear and normal stresses were created by changing the orientation of the specimen with respect to the loading direction. By varying the loading angle, it was possible to create stress biaxiality that included pure tension, mixed tension-shear and pure shear in the significant section of the specimen. The maximum fatigue load in each case was a percentage of the peak load determined in static biaxial loading. The effect of biaxiality ratios on fatigue life diagrams and fatigue damage evolution in the composite laminate is presented.

## 1 INTRODUCTION

Fiber reinforced polymer composites are used in many different structural forms and applications in aircraft, space, automotive, marine and multiple other industries owing to their high strength-to-density and high modulus-to-density ratios. Their fatigue behavior under uniaxial loading has received much more attention compared to biaxial loading [1-3]. Majority of the test data corresponding to biaxial static and fatigue performance that exist in the open literature have come mainly from three types of test specimens [4, 5]: 1) off-axis specimens, 2) cruciform specimens, and 3) thin-walled tubular specimens. Of the three types of test specimens, only thin-walled tubular specimens can be used to apply a combination of normal stresses and shear stress. The normal stresses are created by the application of either an internal pressure or an axial load, and the shear stress is created by the application of a torsional load [6 – 8]. Though tubular specimens have the advantage of allowing biaxial loading, it has many unique challenges, such as tubular specimen fabrication, non-uniform stress distribution through the thickness and the possibility of failure by torsional buckling. The effect of the combination of normal and shear stresses on laminated composite plates has not been studied much in the past. Since the majority of composites are used in laminated plate or shell structures, this study was undertaken to determine the fatigue life diagrams of a continuous fiber reinforced polymer laminate under a combination of normal and shear loadings. The test method used in this study is a butterfly-shaped Arcan specimen, which is a modified form of the Arcan specimen originally developed in 1978 by Arcan and his co-workers [9] and used later to determine the shear properties of fiber reinforced polymers [10]. The versatility of the Arcan specimen is that it can be utilized for testing materials under either normal loading, shear loading or a combination of in-plane normal and shear loadings.

## 2 EXPERIMENTAL

### 2.1 Material

The material used in this study is an E-glass fiber reinforced epoxy flat laminate composed of 13 layers and has a stacking sequence described by  $[0/90/0_4/\bar{0}]_s$ . One layer from each of the outer surfaces of the laminate contains fibers in the transverse direction, but the fibers in the remaining 11 layers are oriented in the longitudinal direction. The trade name for the material is Scotchply 1002. The Scotchply

laminates were originally developed by 3M and is now available by the trade name Cyply 1002 from Red Seal Electric Co. in USA. The nominal fiber volume fraction in the laminate is 64 percent. The longitudinal tensile modulus and strength, as reported by the laminate manufacturer, are 39.3 GPa and 965.3 MPa, respectively.

## 2.2 Fatigue Specimens

The overall dimensions of the butterfly-shaped Arcan specimen used in this study are 50 mm x 75 mm x 3.3 mm (thickness). The notch radius at the corner of the 90° notch angle is 10 mm. The details of the specimen design are given in Reference [11]. The distance between the notch ends is 23.28 mm; thus the cross-sectional area of the specimen between the notch tips, considered the significant section, is 76.82 mm<sup>2</sup>. The specimen has three 6-mm diameter bolt holes drilled at each end for mounting it to the loading fixture. Two different specimen configurations were prepared: 1) longitudinal specimens in which the 0° layers are perpendicular to the significant section, referred to as ‘1-2 specimens’, and 2) transverse specimens in which the 0° layers are parallel to the significant section, referred to as ‘2-1 specimens’. Figure 1 shows a schematic of the 1-2 and 2-1 specimens. In this figure, the 0° layers are represented by the solid lines and the 90° layers are represented by the dotted lines. In the 1-2 specimens, 11 of the 13 layers or 85% of the layers are the 0° layers. Similarly, in the 2-1 specimens 11 of the 13 layers or 85% of the layers are the 90° layers. In addition to 1-2 and 2-1 specimens, 30° and 45° off-axis specimens were also considered. The laminate configurations in the off-axis specimens are [30/60/30<sub>9</sub>/60/30] and [45/-45/45<sub>9</sub>/-45/45], respectively.

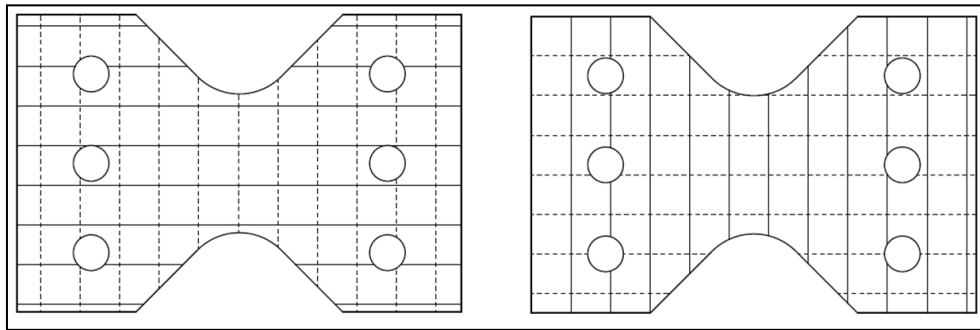


Figure 1: Fiber orientation on the outer surfaces shown by solid lines in 1-2 (left) and (b) 2-1 (right) configurations of the Arcan specimen

## 2.3 Fatigue Tests

Load-controlled cyclic fatigue tests were conducted on an MTS 810 servo-hydraulic test system. The fixture for testing the Arcan specimens is shown in Figure 2 and is described in Reference [11]. It is to be noted that as the loading angle  $\alpha$  is increased from 0 to 90°, the shear stress component increases while the normal stress component decreases. In our experiments, the normal stress component for the 1-2 specimens is  $\sigma_{11}$  and for the 2-1 specimens, it is  $\sigma_{22}$ .

All fatigue tests were performed in load-controlled mode at 2 Hz and with an R-ratio ( $P_{\min}/P_{\max}$ ) of 0.1. The maximum cyclic loads applied on the fatigue specimens were 28 to 76% of the peak load observed in monotonic tests [11]. The load and crosshead displacement signals were continuously monitored and recorded throughout the tests. The cycle at which the instantaneous stiffness (load divided by crosshead displacement) becomes equal to half the stiffness at 100 cycles was considered the failure cycle for the material. If a specimen did not fail, the fatigue test was discontinued after a *runout* life of  $2 \times 10^6$  cycles.

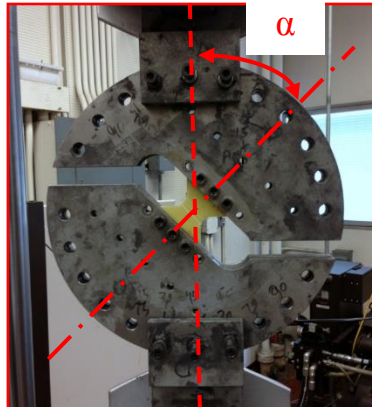


Figure 2: Photograph of an Arcan specimen mounted on the test fixture. The loading angle is denoted by  $\alpha$  and is measured from the vertical axis of the loading fixture.

### 3. FATIGUE LIFE DIAGRAMS

In reporting load-controlled uniaxial fatigue data, it is customary to plot the fatigue life diagram using the maximum normal stress instead of maximum load as the fatigue parameter. In biaxial fatigue tests, there are two in-plane normal stresses,  $\sigma_{xx}$  and  $\sigma_{yy}$ , and a shear stress,  $\tau_{xy}$ . The effects of all three stresses are represented by the normal and shear stress biaxiality ratios defined below. Table 1 lists the biaxiality ratios for the specimen configurations used in this study.

(1) For the 1-2 specimens,

$$\lambda_y = \frac{\sigma_{yy}}{\sigma_{xx}} \quad \text{and} \quad \lambda_{xy} = \frac{\tau_{xy}}{\sigma_{xx}} \quad (1)$$

(2) For the 2-1 specimens,

$$\lambda_x = \frac{\sigma_{xx}}{\sigma_{yy}} \quad \text{and} \quad \lambda_{xy} = \frac{\tau_{xy}}{\sigma_{yy}} \quad (2)$$

Specimen Configuration	Loading angle, $\alpha$ (°)	$\lambda_y$	$\lambda_{xy}$	Specimen Configuration	Loading angle, $\alpha$ (°)	$\lambda_x$	$\lambda_{yx}$
1-2	30	0	0.58	2-1	0	0	0
	45	0	1		30	0	0.58
	60	0	1.73		45	0	1
	90	0	$\infty$		60	0	1.73
30° Off-Axis	0	0.33	0.57		90	0	$\infty$
45° Off-Axis	0	1	1	30° Off-Axis	0	3	1.73
				45° Off-Axis	0	1	1

Table 1: Test configuration and biaxiality ratios of 1-2 and 2-1 Arcan specimens

Figures 3 and 4 show the semi-log plots of the maximum normal stress component acting on the 1-2, 2-1 and off-axis specimens are plotted along the y-axis and the number of cycles to failure along the x-axis. The 1-2 and 2-1 specimens were tested at various loading angles listed in Table 1, whereas the off-axis specimens were tested at 0° loading angle. Since the maximum normal stress  $\sigma_{xx}$  for 1-2 specimens tested at 90° loading angle is zero, the data points for this angle lie on the x-axis instead on a

fatigue curve. The same is true for 2-1 specimens for which the maximum normal stress  $\sigma_{yy}$  is zero when it was tested at  $90^\circ$  loading angle. Figure 3 shows that for  $\lambda_y = 0$ , the fatigue performance is reduced as  $\lambda_{xy}$  is increased. By comparing the fatigue curves corresponding to  $\lambda_y = 0, 0.33$  and  $1$ , it can also be observed that the fatigue performance is reduced as  $\lambda_y$  is increased. Similar observations can be made in Figure 4. Thus, increasing normal stress biaxiality and shear stress biaxiality have adverse effects on the fatigue performance of the composite laminate considered here.

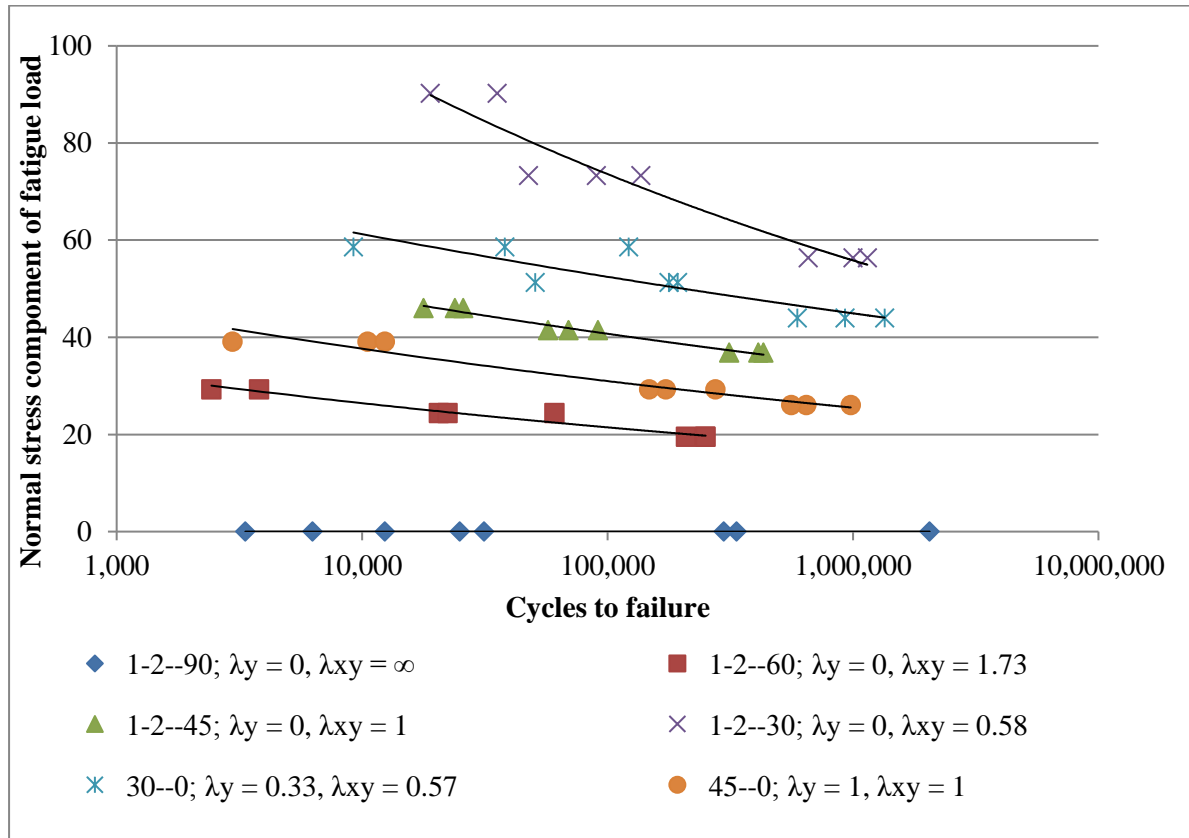


Figure 3: Fatigue life diagrams of 1-2, 30 and  $45^\circ$  off-axis specimens based on the normal stress component  $\sigma_{xx}$ .

#### 4 FATIGUE DAMAGE

Figure 5 shows the fatigue damage on the surfaces of 1-2 and 2-1 specimens tested at  $30^\circ$  loading angle. It is seen that cracks on both specimen surfaces followed the respective fiber direction on the surface. There was also considerable delamination surrounding these cracks. Fatigue damage accumulated on 1-2 specimen surfaces contain longitudinal shear cracks and delaminations along the fiber lengths. The majority of the fatigue damage accumulation occurred in the gage section and there is evidence of slight shear buckling of the  $0^\circ$  fibers. There were also damages at two diagonally opposite areas where the notch radius meets the slanted side of the specimen. The fatigue-tested 2-1 specimens also exhibit multiple shear cracks and slight delamination along their lengths. Like the 1-2 specimens, the 2-1 specimens also have damage that originated from the two diagonally opposite areas where the notch radius meets the slanted side of the specimen. Figure 6 shows the fatigue damage on the surfaces of 30 and  $45^\circ$  off-axis specimens loaded at  $0^\circ$  loading angle. Here also the fatigue damage on the surfaces is mainly in the form of shear cracks in the direction of fiber orientation angle on the surfaces and delamination surrounding these shear cracks.

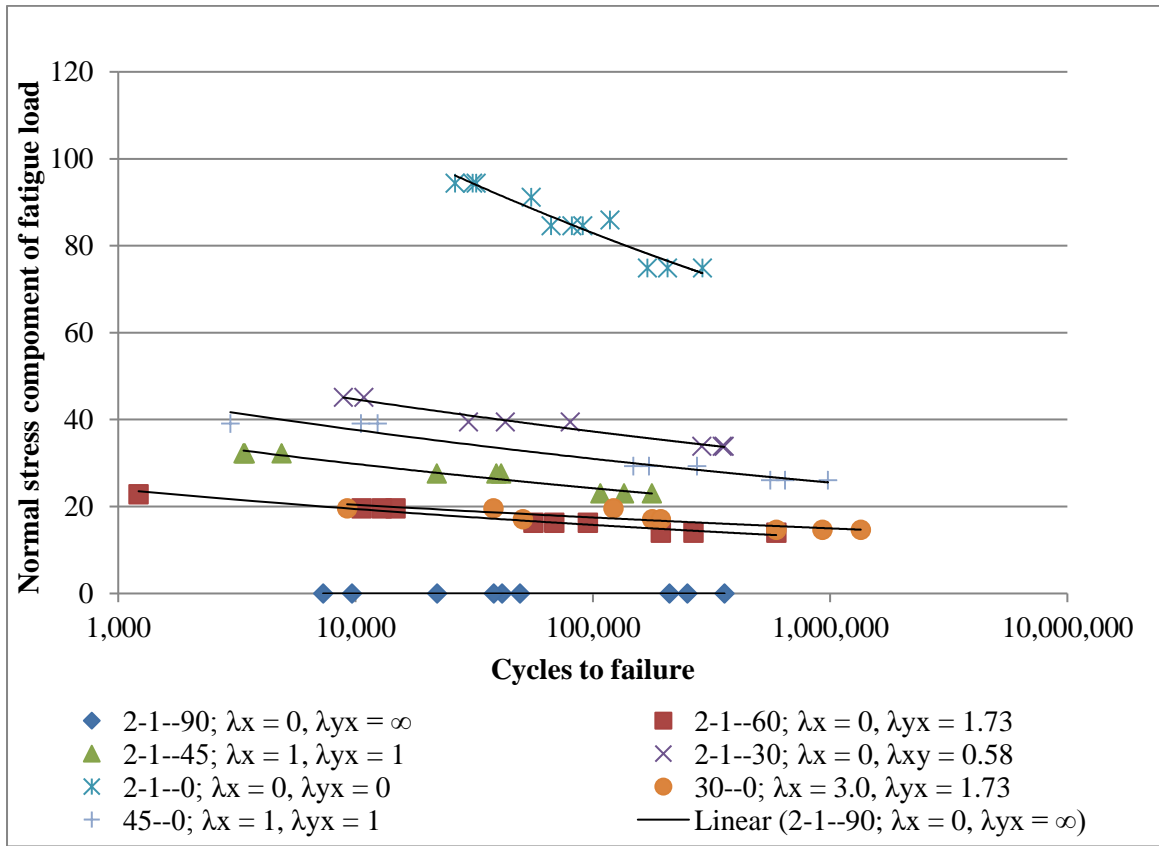


Figure 4: Fatigue life diagrams of 2-1, 30 and 45° off-axis specimen configurations based on normal stress component  $\sigma_{yy}$ .

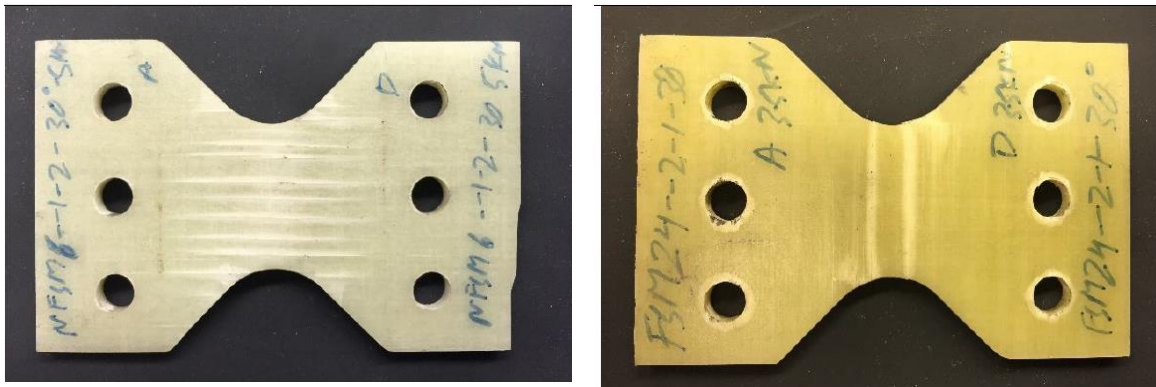


Figure 5: Fatigue damage on the surfaces of 1-2 (left) and 2-1 (right) specimens tested at 30° loading angle



Figure 6: Fatigue damage on the surfaces of 30° (left) and 45° (right) off-axis specimens tested at 0° loading angle

### 5 STIFFNESS DEGRADATION

During load-controlled cycling of fatigue specimens, the instantaneous stiffness defined by the ratio of the maximum load and the maximum displacement decreased due to increase in the maximum displacement. This phenomenon, known as stiffness degradation, occurred due to continuous accumulation of damage in the specimens with increasing number of cycles. Figure 7 shows stiffness degradations in 1-2 specimens tested at a 30° loading angle. In this figure, the maximum cyclic stiffness is defined as the ratio of the maximum cyclic load and the displacement at the maximum cyclic load. For all specimen configurations, the stiffness degradation can be divided into two regions: 1) slow and progressive stiffness degradation, followed by 2) fast and accelerating stiffness degradation. The change from slow and progressive to fast and accelerating stiffness degradation occurs at a knee. Even though there is large amount of scatter, it appears that the higher the maximum fatigue load, the higher is the fatigue degradation. The rate of stiffness degradation in the slow and progressive region is also higher with increasing fatigue load.

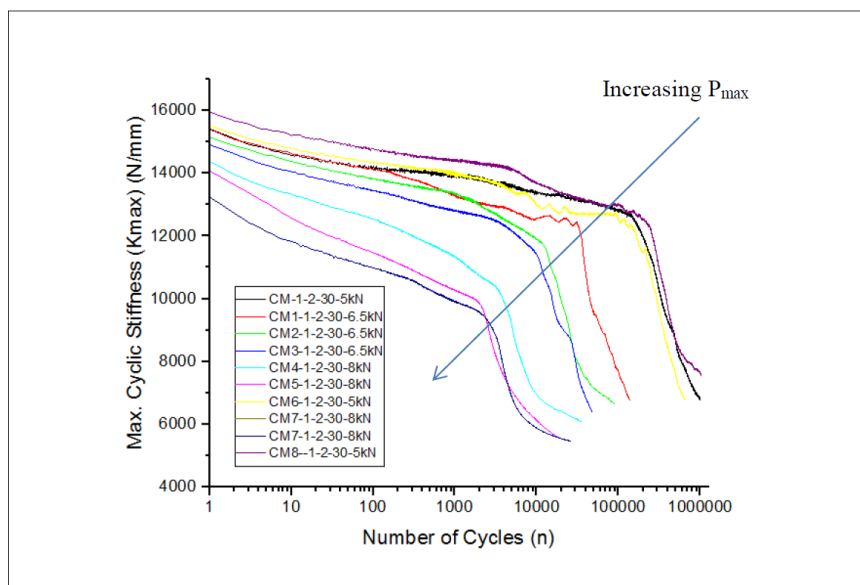


Figure 7: Maximum cycle stiffness as a function of number of cycles (1-2 specimen, loading angle is 30°)

## 6 CONCLUSIONS

In this study, a butterfly shaped Arcan specimen was used for biaxial fatigue testing of an E-glass fiber reinforced epoxy laminate under combined normal and shear loadings. Several different specimen configurations and loading angles were used to develop fatigue failure diagrams with different levels of stress biaxiality. It is observed that increasing shear stress biaxiality decreases the fatigue performance of the laminate. Increasing normal stress biaxiality also decreases the fatigue performance. Under combined loading, fatigue damage was predominantly by shear failure. Stiffness degradation analysis shows that the material displays a knee region before which the stiffness decrease is gradual and slow, whereas upon reaching the knee region the material displays a fast decrease in the stiffness.

## REFERENCES

- [1] B. Harris, Ed., *Fatigue in composites: science and technology of the fatigue response of fibre-reinforced plastics*, CRC Press, Boca Raton, 2003.
- [2] A. P. Vassilopoulos and T. Keller, *Fatigue of fiber-reinforced composites*, Springer, London, 2011.
- [3] A. P. Vassilopoulos, *Fatigue life prediction of composites and composite structures*, Woodhead Publishing, Oxford, 2010.
- [4] M. Quaresimin, L. Susmel, and R. Talreja, "Fatigue behaviour and life assessment of composite laminates under multiaxial loadings," *International Journal of Fatigue*, **32**, 2010, pp. 2-16.
- [5] M. Quaresimin, "50th Anniversary Article: Multiaxial Fatigue Testing of Composites: From the Pioneers to Future Directions," *Strain*, **51**, 2015, pp. 16-29.
- [6] E. W. Smith and K. J. Pascoe, "Biaxial fatigue of a glass-fibre reinforced composite. Part 1: Fatigue and fracture behaviour," in *Biaxial and Multiaxial Fatigue (EGF 3)*, M. W. Brown and K. J. Miller, Eds. Mechanical Engineering Publications, London, 1989, pp. 367-396.
- [7] S. Amijima, T. Fujii, and M. Hamaguchi, "Static and fatigue tests of a woven glass fabric composite under biaxial tension-torsion loading," *Composites*, **22**, 1991, pp. 281-289.
- [8] D. Qi and G. Cheng, "Fatigue behavior of filament-wound glass fiber reinforced epoxy composite tubes under tension/torsion biaxial loading," *Polymer Composites*, **28**, 2007, pp. 116-123.
- [9] M. Arcan, Z. Hashin and A. Voloshin, A method to produce uniform plane stress states with applications to fiber-reinforced materials, *Experimental Mechanics*, **18**, 1978, pp. 141-146.
- [10] A. Voloshin and M. Arcan, Pure shear moduli of unidirectional fibre-reinforced materials (FRM), *Fibre Science & Technology*, **13**, 1980, pp. 125-134.
- [11] R. Mandapati and P. K. Mallick, A study on the biaxial fatigue of E-glass/epoxy laminates under normal and shear loadings, Proceedings of the 20<sup>th</sup> International Conference on Composite Materials, Copenhagen, 2015.